Synaptic Targets of Circadian Clock Neurons Influence Core Clock Parameters

Eva Scholz-Carlson[1,2], Aishwarya Ramakrishnan Iyer[1], Aljoscha Nern[3], John Ewer[4,5], Maria P. Fernandez[1,2,*]

1- Department of Biology, Indiana University Bloomington. Bloomington, 47401 IN
2- Department of Neuroscience and Behavior, Barnard College. New York City, 10027 NY
3- Janelia Research Campus, Howard Hughes Medical Institute, Ashburn VA 20147
4- Instituto de Neurociencia, Universidad de Valparaíso, Valparaíso 2360102, Chile
5- Centro Interdisciplinario de Neurociencias de Valparaíso, Universidad de Valparaíso, Valparaíso 2360102, Chile

* Corresponding author: fernanm@iu.edu

Neuronal connectivity in the circadian clock network is essential for robust endogenous timekeeping. In the *Drosophila* circadian clock network, four pairs of small ventral lateral neurons (sLN_vs) serve as critical pacemakers. Peptidergic communication via sLN_v release of the key output neuropeptide *Pigment Dispersing Factor* (PDF) has been well characterized. In contrast, little is known about the role of the synaptic connections that sLN_vs form with downstream neurons. Connectomic analyses revealed that the sLN_vs form strong synaptic connections with a group of previously uncharacterized neurons, SLP316. Here, we show that silencing synaptic output in the SLP316 neurons via tetanus toxin (TNT) expression shortens the free-running period, whereas hyper-exciting them by expressing the Na[+] channel NaChBac results in period lengthening. Under light-dark cycles, silencing SLP316 neurons also causes lower daytime activity and higher daytime sleep. Our results revealed that the main postsynaptic partners of the *Drosophila* pacemaker neurons are a non-clock neuronal cell type that regulates the timing of sleep and activity.

Keywords: circadian rhythms, connectomics, behavior, neuronal circuits

Introduction

Circadian rhythms, which allow animals to adapt to day-night changes in their environment, are generated by small groups of neurons in the brain that contain molecular clocks (1). These neurons form a network with synchronized molecular oscillations (2, 3). The maintenance of robust and coherent behavioral circadian rhythms depends on connectivity within the clock network, which controls the timing of key behavioral outputs like rhythms in feeding, mating, and sleep (3). In both mammals and flies, connectivity in the clock network is mediated by peptide and transmitter outputs (4-7). Although the molecular mechanisms driving endogenous oscillations in clock neurons are well described, the pathways through which these neurons communicate with each other and with downstream targets to propagate oscillations throughout the brain remain poorly understood.

Drosophila melanogaster is an ideal model for studying connectivity in the clock network. The fly circadian network consists of ~240 neurons ((8), reviewed in (9)) and is the functional equivalent of the mammalian suprachiasmatic nuclei, the principal clock in the vertebrate brain (10, 11). Each clock neuron within this network has an intracellular molecular timekeeping mechanism based on a transcriptional–translational feedback loop (12). Clock neurons can be organized into seven main groups based on their anatomical location (11, 13-16). Whereas the molecular oscillations of most of these groups are in phase, some major clock groups become active at specific times of day, which correlates with their roles in behavioral outputs (17). Among these cells, the small lateral ventral neurons (sLN_vs) are key for maintaining rhythmicity under conditions of constant darkness and temperature (DD) and are considered the dominant circadian pacemakers under these conditions (18-21). Despite the importance of these cells for sustaining physiological and behavioral rhythms, very little is known about their connectivity with target neurons. Indeed, an analysis of their synaptic connectivity revealed that they form very few monosynaptic connections with other clock neurons (16).

Peptidergic signaling is essential for clock network intercommunication and output (6). The neuropeptide *Pigment Dispersing Factor* (PDF), which is secreted by the sLN_vs, is required for synchronizing molecular oscillations within the network, setting the phase of neural activity in other groups of clock neurons, and maintaining activity-rest rhythms under constant conditions (18, 22-24). Expression of PDF undergoes daily and circadian oscillations in the sLN_v dorsal terminals (19), and the loss of PDF or of the PDF receptor (PDFR) results in arrhythmicity under free-running conditions (25-27). In addition to PDF, the sLN_vs express the neuropeptide, short Neuropeptide F (sNPF) (28), which promotes sleep and is involved in feeding regulation (28-30), and the inhibitory neurotransmitter glycine (31). Interestingly, downregulation

of *bruchpilot* (*brp*) and of other synaptic active zone proteins expressed by the sLN_vs does not affect rhythmicity, and dense-core vesicle release profiles of the sLN_vs in the Full Adult Fly Brain (FAFB) do not show spatial overlap with BRP-labeled active zones (32). This finding is consistent with the observation that neuropeptide release takes place from sites located all along the sLN_v, including the soma (33), and with the persistence of robust behavioral rhythmicity upon silencing of synaptic transmission (34) in *Pdf*+ neurons (35, 36)

Although the circadian clock provides predictability, it must also be flexible to adapt to varying environmental conditions. Distinct subsets of neurons control the morning and evening bouts of activity that produce the bimodal pattern that flies show under light-dark cycles. The sLN_vs, which are active around dawn (17), are associated with the morning peak of activity (18, 20, 21) and are called morning (M) cells. The PDFR-expressing lateral neurons dorsal (LN_ds) and the PDF-negative 5th LN_v are associated with the evening peak activity (20, 21, 37) and their neural activity peaks before dusk (17). Some dorsal neurons (DNs) also contribute to the timing and amount of activity and sleep via the modulation of M and E cells (38-41). The phase of the morning and evening activity bouts adjusts to environmental light and temperature (42-47), allowing flies to adjust their activity patterns according to the season.

The four sLN_vs form few direct synaptic connections with other clock neurons or with other neurons outside the clock network, yet they form strong connections with a previously uncharacterized group of neurons named SLP316. The SLP316 cells synapse onto the DN1pA class of dorsal clock neurons, which are associated with the reorganization of sleep/wake cycles (reviewed in (40)). Here, we show that despite not being clock neurons themselves, silencing SLP316 neuronal activity resulted in a shortening of the free-running period of activity, whereas their excitation resulted in the opposite phenotype. Neither manipulation led to the loss of rhythmicity. Under light-dark cycles (LD), manipulations of the SLP316 activity led to a reduction in evening activity and an increase in sleep, both under ambient temperature of 25°C, and under cold, winter-like days. Under both LD and DD, the behavioral phenotypes observed were different from those caused by the loss of PDF. In conclusion, our data reveal a role for a previously unknown neuronal population that connects two classes of clock neurons but is not itself part of the circadian clock network, in regulating the timing of sleep/wake cycles.

Results

1-Connectomics datasets identify SLP316 neurons as primary post-synaptic partners of sLN_vs

101 Based on the *Drosophila* hemibrain connectome (48), the sLN_vs form much stronger connections with an
102 uncharacterized neuronal cell type than with any other neurons, including other clock neurons (16) (Fig.
103 1A). This cell type, SLP316, consists of three neurons with somas in the dorsal-most region of the Superior
104 Lateral Protocerebrum (SLP) (48). Interestingly, the sLN_vs are in turn the main presynaptic inputs to
105 SLP316 neurons (Fig 1A, B). Most inputs to SLP316 cells from their top ten presynaptic partners are located
106 along the ventromedial projections, whereas their output synapses are concentrated along the dorsal
107 arborizations (Fig. 1C).
108
109 The synapses formed by the sLN_vs onto the SLP316 neurons represent 70% of the synapses by all groups
110 that form strong connections with these cells (weight >10) (Fig 1A, B). Many of the synapses that the sLN_vs
111 form onto the SLP316s (~20%) are located below the point at which the sLN_vs extend and ramify their
112 dorsal termini (Suppl. Fig. 1A), the region long thought to be the location of sLN_v output synapses. The
113 other main inputs to SLP316 are from two neurons that belong to the SLP364 cell type and from
114 ventroposterior (VP) antennal lobe glomeruli neurons. The SLP316s are innervated largely by neurons in
115 the SLP neuropil but also from the superior medial (SMP) and posterior lateral (SLP) protocerebrum (Suppl.
116 Fig. 1B).
117
118 The SLP316 neurons are largely homogeneous in their connectivity patterns with upstream neurons, but
119 their outputs are more varied (Fig 1B'). These cells form some of the strongest connections with another
120 group of clock neurons, posterior dorsal neurons (DN1p). The DN1pA class of clock neurons is the top
121 output of the SLP316 cells. The main neuropil innervated by SLP316s is the SLP, followed by the SMP
122 and PLP with a much smaller number of connections (Suppl. Fig. 1B). We next examined the connectivity
123 patterns of the sLN_vs in the FlyWire *Drosophila* connectome (49) to determine whether cells similar in
124 morphology to the SLP316s were among their top post-synaptic partners. We found that in both
125 hemispheres, the sLN_vs form most of their output synapses with cells highly similar in location and
126 morphology (Suppl. Fig. 1C). Computational predictions based on synapse architecture for both the
127 hemibrain and FAFB-Flywire datasets (50) indicate that SLP316 cells are likely glutamatergic.
128
129 **2-The SLP316 neurons are non-clock neurons that extend along the sLN_v projection tract**
130
131 To further study the SLP316 neurons, we generated a Split-Gal4 line that targets these cells (#SS76489, see
132 Methods) (Suppl. Fig. 2A). Since both the hemibrain and FAFB/FlyWire connectomes correspond to an
133 adult female (48), we dissected brains from both *SLP316>mCD8-GFP* males and females to determine if
134 there were sex differences in the number of cells or their morphology. The projections from the SLP316

135 neurons extend toward the ventral brain along the same tract as the projections of the sLN_vs, which extend
136 from the ventral to the dorsal brain (Fig. 2A-B). We did not find expression in additional neurons in the
137 central brain or the ventral nerve cord, or sex differences in the number of cells (Fig. 2C). The number of
138 cells remains similar in older flies (Suppl. Fig. 2B). Therefore, we conclude that the driver is likely
139 specifically expressed in SLP316 neurons in adults and that the expression pattern is similar in males and
140 females.
141
142 The SLP316 neurons are in the dorsoposterior area of the brain, where the DN1ps are located. To determine
143 if these cells were yet unidentified clock neurons, we co-stained with a PER antibody. Adult
144 *SLP316>mCD8-GFP* flies were entrained to a 12h:12h light-dark cycle (LD) for 5 days, and brains were
145 dissected at the end of the night (ZT23), when PER nuclear signal is strongest (51). We did not detect PER
146 nuclear signal in the somas of any of the SLP316 cells (Fig. 2D). Therefore, we conclude that the SLP316
147 neurons are not circadian clock neurons. To determine if there were daily changes in excitability in these
148 cells, we used a transcriptional reporter in which the *Hr38* regulatory DNA is upstream of a nuclear-
149 localized fluorescent Tomato reporter (52). In the sLN_vs, the *Hr38-Tomato* reporter gene shows higher
150 expression around ZT2, consistent with a previous study (53). In contrast, SLP316 cells showed consistently
151 low signal, and the presence of physiological rhythms cannot be excluded based on these data (Suppl. Fig.
152 2C-D).
153
154 Next, we assessed connectivity between the cells labeled by the SLP316 split-GAL4 line and the sLN_vs via
155 BAcTrace. This is a retrograde synaptic tracing technique in which *Clostridium botulinum* neurotoxin A1
156 (BoNT/A) is transferred from a postsynaptic donor cell (driven by Gal4 components) to a presynaptic
157 receiver cell (driven by LexA components) by targeting the interior of a synaptic vesicle (54). In the receiver
158 cell, the toxin releases a membrane-localized transcription factor, inducing Tomato expression. When a
159 vesicle is recycled, the toxin is internalized into the cell. We combined flies expressing the BAcTrace
160 transgenes (see the methods section) with flies carrying both the SLP316 split Gal4 and the *Pdf-LexA*
161 transgenes and stained brains with antibodies against PDF, RFP, and GFP (Fig 2E-H). Experimental flies
162 showed RFP signal in the sLN_vs but not the lLN_vs, whereas PDF-immunoreactivity was detected in both
163 groups of LN_vs (Fig. 2E). Control flies without the SLP316 split Gal4 driver did not express RFP (Fig. 2G).
164 As expected, GFP signal could be detected in both the sLN_vs and lLN_vs in control flies, reflecting the
165 expression pattern of the *Pdf-LexA* driver present in both lines (Fig. 2F and H). We did not observe sex
166 differences in expression pattern in experimental or control flies. These results support the notion that the
167 SLP316 neurons are post-synaptic partners of the sLN_vs, which is consistent with connectomics data.
168

169 **3- Altering the activity of SLP316 neurons changes the free-running period.**

170

171 Elimination of the LN_vs via expression of the pro-apoptotic gene *hid* leads to severe loss of rhythmicity and
172 shortening of the free running period, similar to the behavioral phenotypes of the *Pdf* null mutation,
173 Pdf^{01}(18). Whereas inhibiting synaptic transmission in *Pdf* neurons via tetanus toxin (TNT) does not affect
174 the ability of the flies to maintain rhythmicity in DD, it leads to changes in free-running period, as *Pdf*>TNT
175 flies show longer periods than their parental controls (35, 36). Since the SLP316s are the main cell type
176 downstream of the clock pacemaker neurons, we asked how manipulations of these cells would affect
177 behavioral rhythms.

178

179 The bacterial voltage-gated sodium channel *NaChBac* is used to increase neuronal excitability (reviewed
180 in (55)). Expression of *NaChBac* in *Pdf*+ expressing neurons results in complex rhythms, with multiple
181 superimposed period components under free-running conditions (56). *NaChBac* expression in the SLP316
182 cells resulted in lengthening of the free-running period without affecting overall rhythmicity (Fig. 3A-C
183 and Table 1), similar to the phenotype observed upon silencing activity of the *Pdf*+ neurons via TNT. After
184 eight days in DD, experimental flies showed a 3.3-hour phase delay in their activity peak (Fig. 3D-E).
185 Under a light dark-dark cycle, *SLP316>NaChBac* flies showed a significant reduction in daytime activity
186 (Suppl. Fig. 3A-D).

187

188 Next, we expressed *hid* under the SLP316 driver. Under DD conditions, *SLP316>hid* flies had a short free
189 running period (Fig 3F-G). The overall number of rhythmic flies and their rhythmic power were not affected
190 (Fig 3H and Table 1). A phase advance in activity can be detected on day 8 under DD conditions (Suppl.
191 Fig. 3P-Q). *SLP316>hid* females also show a shortening in free-running period and no effect on the overall
192 number of rhythmic flies (Suppl. Fig. 4A-B and E). Therefore, elimination of most SLP316 cells and
193 *NaChBac*-mediated hyperexcitation of these cells led to opposite phenotypes in free-running period of
194 activity rhythms.

195

196 To determine whether synaptic activity of the SLP316 cells mediates the effects on period we expressed
197 TNT (34). This manipulation led to a shortened period (Fig 3F, I and Table 1). We also observed a small
198 but significant reduction in the percentage of rhythmic flies and a phase advance at DD 8 of ~3.2 hours
199 (Fig. 3J-L). In *SLP316>TNT* females, the reduction in free-running period was not significantly different
200 from that of controls (Suppl. Fig. 4C-E). Under LD, both *hid* and *TNT* expression in SLP neurons resulted
201 in a reduction in daytime activity (Suppl. Fig. 3G, L). Shortening of free-running period is typically
202 associated with an early phase of the evening peak of activity under a light-dark cycle (LD), such as in Pdf^{01}

203 mutants or flies in which *Shaggy* or *Doubletime* (DBT^S) are expressed in the sLN_vs (57, 58). However, LD
204 activity profiles of *SLP316>hid* and *SLP316>TNT* flies indicate that these flies could still anticipate the
205 lights-on transition and did not have an early phase of the evening peak (Suppl. Fig. 3F,I,K and N). The
206 evening peak area in experimental *SLP316>hid* and *SLP316>TNT* males was significantly lower than the
207 controls, indicating lower activity at this time of day (Suppl. Fig.3J,O).
208
209 The only behavioral rhythm that is mediated by the LN_vs but does not rely on PDF is adult emergence from
210 the pupal case (eclosion) (59, 60). The larval LNs, which survive metamorphosis and become the adult
211 sLN_vs (61), communicate with the PTTH neurons to regulate eclosion rhythms (59). In pharate adults, the
212 sLN_vs inhibit PTTH neuron Ca^{2+} activity via short neuropeptide F (sNPF), not PDF, and the PTTH neurons
213 appear to be post-synaptic targets of the sLN_vs based on transsynaptic tracing experiments (59). In addition,
214 PTTH neurons express sNPF and not PDF receptors (59). To determine if manipulations of SLP316 neurons
215 affected eclosion rhythms, we conducted population experiments in which these cells were eliminated via
216 expression of *hid*. We did not detect eclosion rhythm phenotypes in experimental *SLP316>hid* flies (Fig.
217 4A-B). Taken together, these results show that manipulations of the SLP316 neurons affect free-running
218 rhythms in activity but not eclosion rhythms.
219
220 **4.- Organization of activity under cold days is disrupted upon SLP316 silencing**
221
222 Since a subset of the DN1p class of clock neurons are major postsynaptic partners of the SLP316 cells, we
223 investigated the effect of manipulating these cells under low temperature light-dark (LD) conditions, where
224 the DN1ps appear to play a more prominent role in shaping activity (45). Only under conditions with low
225 light intensity, low temperature, or low or absent PDF can rescuing the molecular clock in a subset of
226 glutamatergic DN1ps promote an evening peak of activity (44, 45).
227
228 Low temperatures lead to a reorganization of activity in wild-type flies as they adapt to the shorter days of
229 winter. Under low temperature conditions (18°C) and light-dark cycles, the distance between the morning
230 and evening peaks is reduced, primarily due to a substantially earlier phase of the evening peak, which
231 decreases the phase angle of entrainment (42). We exposed flies in which we eliminated or silenced SLP316
232 cells to LD cycles under cold temperatures. *SLP316>hid* flies show significantly reduced daytime activity
233 and increased daytime sleep compared to controls (Fig. 5A-D). Similar phenotypes, both in terms of
234 daytime activity and daytime sleep, were observed in experimental *SLP316>TNT* flies (Fig. 5E-H). Neither
235 nocturnal activity nor sleep were affected (Suppl. Fig. 5A-D).
236

237 Under free-running conditions, manipulations of SLP316 neuron activity and the loss of *Pdf* result in
238 distinct phenotypes. The *Pdf*^{01} mutant is predominantly arrhythmic (18). However, the *Pdf*^{01}flies that
239 remained rhythmic exhibited a shortened free-running period, similar to the effect observed after silencing
240 SLP316 neurons (18). Under light-dark (LD) conditions, manipulations of SLP316 neurons did not cause
241 the expression of the classic phenotypes associated with the loss of *Pdf*, such as a lack of morning
242 anticipation or an advanced evening peak (Suppl. Fig. 3). The advanced evening peak is thought to result
243 from a phase-delay effect of PDF on evening cells: in the absence of PDF, neuronal activity in the evening
244 cells show a large phase advance (24). PDF levels are temperature-sensitive, increasing during hot, summer-
245 like days and decreasing under colder conditions (62).
246
247 We exposed *Pdf*^{01}flies to the same LD 18°C cycles and observed a significant advance in the evening peak
248 and a 1.5-fold increase in daytime activity (Fig. 5I-J). This indicates that the early peak observed in wild-
249 type flies under LD (42) is not solely attributable to the reduction in PDF under lower temperatures, since
250 flies that lack PDF show a pronounced shift in evening activity. *Pdf* mutants show higher levels of daytime
251 sleep in 12:12 LD cycles at 25°C (63); however, the pronounced increase in evening activity under LD
252 18°C is accompanied by an overall decrease in daytime sleep (Fig. 5K-L). The onset of activity was earlier,
253 and activity levels remained high until the lights-off transition. After the lights-off transition, activity and
254 sleep levels between control and *Pdf*^{01} flies converge (Fig. 5I,K and Suppl. Fig. 6E-F). These findings
255 indicate that under cold-day conditions, the loss of *Pdf* and the silencing or elimination of SLP316 neurons
256 results in the expression of opposite behavioral phenotypes.
257
258 **5.- Silencing SLP316 neurons increases daytime sleep**
259
260 Under standard light-dark conditions at 25°C, *Pdf* mutants show increased sleep during the day, as well as
261 during the subjective day under constant conditions (63). However, the effect of *Pdf* loss on sleep appears
262 to be dependent on temperature: indeed, these flies show increased sleep at 25°C and decreased sleep at
263 18°C (Fig. 5L). We analyzed the sleep profiles of flies expressing *hid* in the SLP316 cells under a LD cycle
264 at 25°C and observed a significant increase in daytime sleep (Fig. 6A-B). (These results were obtained
265 using the standard quantification based on periods of 5 minutes of inactivity (64, 65)). A similar phenotype
266 was observed in *SLP316>TNT* flies (Fig. 6E-F). Neither of those manipulations affected nighttime sleep
267 (Suppl. Fig 6). These findings allow us to conclude that the effects on sleep are not unique to low
268 temperature cycles but, in contrast to PDF's temperature dependent roles, reflect a feature of the SLP316
269 neurons at both low and high temperature.
270

271 To determine the underlying cause for this increase in sleep, we analyzed P(doze) and P(wake), the
272 probabilities that an inactive fly will start moving or an active fly will stop moving, respectively, between
273 1-minute activity bins. P(doze) corresponds to sleep pressure, and P(wake) corresponds to sleep depth; thus,
274 these conditional probabilities can offer insight into the biological processes driving changes in sleep (66).
275 P(doze) was higher throughout most of the day and night for both *SLP316>hid* and *SLP316>TNT* animals,
276 especially during the evening (ZT6-12) and morning (ZT18-3), when flies are most active (Fig. 6 C,D and
277 G,H). The average P(wake) was not significantly affected in either manipulation, although *SLP316>hid*
278 flies showed a minor reduction in P(wake) from ZT9-12 (Suppl. Fig. 7A-D). This increase in P(doze)
279 suggests that the increased sleep observed when the SLP316s are silenced was due to increased sleep
280 pressure, especially at times when flies should be most active. We conclude that silencing SLP316 neurons
281 leads to an increase in daytime sleep under both 25°C and low temperature conditions, and that this
282 phenotype is not dependent on PDF since *Pdf* manipulations lead to opposite effects.
283
284 **Discussion**
285
286 The recent availability of connectomics data allows the identification of neuronal connections that have not
287 been described using other approaches. We used openly available *Drosophila* connectomes to identify the
288 SLP316 neurons, which are the main post-synaptic partners of the sLN_vs, the key pacemaker neurons in the
289 *Drosophila* clock network. We found that genetic manipulations of the SLP316 neurons led to changes in
290 free-running rhythms: silencing their activity via TNT or eliminating them via *hid* leads to a period
291 shortening, whereas hyperexciting them via *NaChBac* led to a period lengthening. Another important
292 behavioral output of the sLN_vs, eclosion rhythm, was not affected by genetic elimination of SLP316
293 neurons. Under light dark cycles, silencing SLP316s resulted in a reduction in daytime activity and an
294 increase in sleep, under both 25°C and low temperature conditions. Neither the free-running nor the light-
295 dark (LD) phenotypes observed following SLP316 manipulations resembled those caused by the loss of
296 PDF, a well-known output of the sLN_vs, which facilitates communication with the rest of the circadian
297 clock network.
298
299 Our study identified a non-clock group of neurons that affects circadian rhythms and contributes to our
300 understanding of neuronal connectivity within the clock network. To date, the best characterized output of
301 the sLN_vs is PDF (18, 67), a neuropeptide that accumulates--and is also released (33)- rhythmically from
302 their dorsal termini and soma, likely independently of classical transmitter release from these cells (32).
303 The sLN_vs also express sNPF (28), and there is evidence that they also use glycine to communicate with
304 postsynaptic targets (31). Based on the availability of neurotransmitter use information, the flywire EM

305 prediction for the sLN_vs is acetylcholine (50), but the likelihood is relatively low. If the sLN_vs contact the
306 SLPs via glycine, they would likely inhibit them, which is consistent with the observation that inhibiting
307 synaptic release from *Pdf* neurons via TNT and exciting the SLP316 neurons via *NaChBac* both lead to
308 period lengthening. Functional connectivity experiments between the sLN_vs and the SLPs would be needed
309 to determine the nature of this connection.
310
311 Given their prominent role in the clock network, several studies have examined neuronal targets of the
312 sLN_vs that would contribute to the propagation of rhythmic signals throughout the brain. PDF receptors
313 (*PdfR*) are expressed by a wide range of neurons distributed throughout the brain, including much of the
314 clock network (6), and PDFR-expressing cells respond to sLN_v stimulation (68). PTTH neurons, which are
315 downstream of sLN_vs, express sNPF receptors, are inhibited by the sLN_vs via sNPF to regulate eclosion
316 rhythms (59). Connections between *Pdf*+ cells and non-clock cells that regulate rhythm amplitude were
317 detected via GRASP (69). More recently, the Blau laboratory used the transsynaptic tracer trans-tango to
318 identify neuronal populations downstream of the sLN_vs and reported that they form connections with a
319 subset of DN1p clock neurons that express the neuropeptide CNMa and with mushroom body Kenyon cells
320 (70). Strong monosynaptic connections between the sLN_vs and the DN1ps cannot be detected in the
321 connectomes (16, 49), but it is possible that those synapses were missed because the sLN_vs show daily
322 structural plasticity rhythms (71), as do the VIP expressing neurons in the SCN (72). Truncation of the
323 dorsal termini of the sLN_vs, which are the sites of synaptic output and undergo clock-controlled plasticity,
324 does not affect free-running rhythms (38, 73), suggesting that PDF release is independent of the arborization
325 rhythms. In addition, silencing synaptic transmission in *Pdf*+ neurons via TNT does not lead to the loss of
326 behavioral rhythms (36), nor does downregulation of *bruchpilot* (*brp*) or other active zone proteins (32).
327 Taken together, these results suggest that unlike PDF release, the synaptic connections that the sLN_vs form
328 with downstream neurons are not required for maintaining activity-rest rhythms under free running
329 conditions. However, those connections play a role in regulating the free-running period of those rhythms.
330
331 The sLN_vs appear to contact the DN1p clock neurons both via PDF release (58) and synaptically through
332 the SLP316s (Fig. 1). A functional clock in CRY-positive DN1ps, along with the presence of PDF, is
333 sufficient for morning anticipation (44, 45, 74). Neither inhibition of synaptic transmission from sLN_v nor
334 manipulation of the SLP316 cells appeared to affect morning anticipation, suggesting that this feature
335 depends on only PDF signaling from the sLN_vs. Rescuing the molecular clock in a glutamatergic subset of
336 DN1ps can promote an evening peak of activity when PDF is reduced or absent (44, 62). The pronounced
337 and very early peak of activity we observed in Pdf^{01} flies under cold temperatures may at least in part be
338 due to increased prominence of the activity of evening DN1ps in the absence of PDF (75). Another clock

339 subset, DN1a, which is inhibited by cold temperature, is connected reciprocally to the sLN_vs through the
340 neuropeptides CCHamide1 and PDF (76, 77). Thus, a cold-temperature induced change in sLN_v activity
341 could alter evening DN1p activity via the SLP316s, while simultaneous loss of PDF eliminates suppression
342 of the DN1p-induced effects. These glutamatergic DN1ps are also sleep-promoting; activating them
343 increases daytime sleep and arousal threshold at ZT6 and 10, whereas inhibiting them decreases both
344 daytime and nighttime sleep (78). If the SLP316 neurons are glutamatergic as predicted in Flywire (49) and
345 inhibitory, silencing them would be expected to increase the neuronal activity of the DN1ps and thus
346 daytime sleep levels, in agreement with our results.
347
348 Studying how neurons use different signals to communicate with downstream targets is essential for
349 understanding how networks of neurons produce behavior. The *Drosophila* sLN_vs are an excellent model
350 for studying neuronal basis of behavior given their well characterized role as key circadian pacemakers.
351 This role relies on their release of the neuropeptide PDF as a critical output signal for synchrony within the
352 network. Our study is the first to examine the role on rhythmic behavior of direct synaptic targets of the
353 sLN_vs based on connectomics data, a connection that is likely independent of PDF. Our results reveal that
354 manipulations of the SLP316 cells, the primary postsynaptic partners of the sLNvs in the connectome, can
355 affect a core circadian parameter, free-running period. This finding indicates that a non-clock neuronal cell
356 type can modulate circadian timekeeping. We show that manipulations of the SLP316 cells and loss of PDF
357 lead to different behavioral phenotypes, both under free running conditions and under standard and low
358 temperature light-dark cycles. These two pathways of clock neuron output may add plasticity to the system
359 and allow the circadian network to adjust to changing environmental conditions.

360 **Materials and Methods**

361 **Fly lines and husbandry:**
362 Flies were reared on cornmeal-sucrose-yeast media under a 12hr:12hr Light:Dark (LD) cycle at 25 °C. The
363 fly lines used in this study were: *SLP316 split-Gal4* (SS76489: w; 38E08-p65ADZp in attP40; 36B07-
364 ZpGdbd in attP2), *w*; *Pdf-Red, Pdf-Gal4; w;;UAS-NaChBac, yw;UAS-hid/cyo;UAS-mCD8-GFP, w;UAS-*
365 *TeTxLC;*, w^{1118}, *w;;*Pdf^{01}, and *w;* LexAop2-Syb.GFPN146I.TEVT173V LexAop2-
366 QF2.V5.hSNAP25.HIVNES.Syx1A/CyO,20XUAS-B3R.PEST-UAS(B3RT.B2)BoNTA QUAS-
367 mtdTomato-3xHA/TM6B, Tb1 (see Fly Lines and Reagents table for details).
368
369 We identified the SLP316 split-GAL4 line (SS76489) by screening candidate hemidriver combinations
370 selected by comparing GAL4 driver expression patterns and the hemibrain reconstructions of SLP316. This

371 work was done in collaboration with the Janelia Fly Light Project Team using established methods and the
372 driver line is included in a recently published split-GAL4 collection (79).
373
374 **Immunohistochemistry:**
375 Flies were entrained to 12:12 LD cycles at 25°C and dissected at the specified times in cold Schneider's
376 *Drosophila* Medium. For all experiments, dissections were completed within 30 minutes. For anti-PER
377 staining (Fig. 2D), brains were dissected at ZT23 on the fifth day under LD. Brains were fixed in 2%
378 paraformaldehyde prepared in Schneider's *Drosophila* Medium for 30 minutes at room temperature.
379 Blocking was performed using 5% normal goat serum in PBS containing 0.3% Triton (PBS-TX) for 1 hour
380 at room temperature. Samples were incubated with primary antibodies for 24 to 48 hours at 4°C, followed
381 by several washes with PBS-TX under agitation. Secondary antibody cocktails were applied for 24 to 48
382 hours at 4°C, after which samples were washed again with PBS-TX. Antibodies (see table) were diluted in
383 PBS-TX supplemented with 5% normal goat serum. Brains were mounted between coverslips and imaged
384 at the Advanced Science Research Center (GC-CUNY) using an Olympus Fluoview 3000 laser-scanning
385 confocal microscope (Olympus, Center Valley, PA). Brains for the BacTrace experiments were imaged
386 using an Olympus/Evident Fluoview 4000 laser-scanning confocal microscope (Fernández lab, Indiana
387 University Bloomington).
388
389 The LM images in Figure S2 are based on confocal stacks previously reported (79) and the original images
390 are available online (https://splitgal4.janelia.org/cgi-bin/view_splitgal4_imagery.cgi?line=SS76489). The
391 EM-LM overlay was generated using VVDviewer (https://zenodo.org/records/14468001). The other
392 images show maximum intensity projections produced using Fiji (https://imagej.net/software/fiji/).
393
394 **Connectome analysis:**
395 The *Drosophila* Hemibrain (release v2.1) was accessed via neuprint (https://neuprint.janelia.org/). FlyWire
396 data are based on FAFB version 783 (https://flywire.ai/)(49, 80). Hemibrain reconstructions are identified
397 by their instance names in neuprint (e.g. 'SLP316_R') with individual cells distinguished here by an
398 additional number ('SLP316_R_1').
399
400 **Behavior recording and analysis:**
401 Locomotor activity rhythms of adult male and virgin female flies were recorded using DAM2 *Drosophila*
402 Activity Monitors. Three- to six-day old flies were placed individually in TriKinetics capillary tubes
403 containing 2% agar- 4% sucrose food at one end sealed with a cap, plugged with a small length of yarn,
404 and loaded into the DAM2 monitors for locomotor activity recording. Flies were entrained to 12:12 LD

405 cycles for at least five days and then released into constant darkness (DD) for at least nine days at a constant
406 temperature of 18 or 25°C (as indicated in the figure legend for each experiment).
407
408 Free-running activity rhythms were analyzed with ClockLab software. ClockLab's Chi-square periodogram
409 function was used to analyze rhythmicity and rhythmic power in individual flies using 30-minute bins for
410 activity and a confidence level of 0.01. The "Rhythmic Power" for each designated rhythmic fly was
411 determined by subtracting the "Significance" value from the "Power" value associated with the predominant
412 peak. Flies that did not exhibit a Rhythmic Power of 10 were categorized as "arrhythmic," and their period
413 and rhythmic power were not included in the analysis (81). ClockLab periodogram analysis was repeated
414 for rhythmic flies using 1-minute bins to quantify free-running period. For each of the genotypes tested,
415 only periodicities falling within the 14 to 34-hour range were taken into consideration. Phases on the eighth
416 day of free-running were calculated using 1-minute bins and applying a Least Squares sine-wave fit in the
417 ClockLab activity profile, excluding any phases with $P>0.05$. All relevant information about statistical
418 analyses is included in Table S1.
419
420 Activity counts were collected in 1-minute bins, and averaged across the population and profiles of specific
421 genotypes under LD were generated using PHASE (82). First, individual fly activity levels were normalized
422 by establishing the average activity across all 30-minute bins over days 2-4 under LD. Population averages
423 of this normalized activity were computed for each 30-minute bin and averaged into a single representative
424 24-hour day. Total daytime (ZT0-12) and nighttime (ZT12-24) activity counts from days 2-4 of LD were
425 recorded. Representative sleep plots and amounts were similarly generated for LD days 2-4 by classifying
426 5-minute periods of inactivity as sleep, unless otherwise specified. Total daytime and nighttime sleep over
427 the three-day period were also recorded. Morning and evening phase were quantified in PHASE using a
428 filter frame length of 481 minutes and filter order of 2. P(wake) and P(doze) values (66). were averaged for
429 the entire duration of LD days 2-4, or in three-hour windows and averaged across the same days.
430
431 **Adult emergence monitoring**
432
433 Flies were raised at 25°C for 5 days, then transferred to 20°C and entrained under a LD 12:12 light:dark
434 cycle. Resulting pupae were collected and fixed on eclosion plates with Elmer's glue and mounted on
435 Trikinetics eclosion monitors (Trikinetics, MA, USA). Emergence was then monitored for 7 days at 20°C
436 under DD conditions and analyzed as previously described (83). Rhythmicity of eclosion profiles was
437 analyzed using MATLAB (MathWorks, Inc., Natick) and the appropriate MATLAB toolbox (84). Using

438 autocorrelation analyses, records were considered rhythmic if the rhythmicity index (RI) was 0.3, weakly
439 rhythmic if 0.1<0.3, and arrhythmic if RI<0.1 (20).
440
441 **Fly lines and reagents**
442

REAGENT or RESOURCE	SOURCE	IDENTIFIER
Experimental Models: Organisms/Strains		
SLP316 split Gal4 (w; 38E08-p65ADZp in attP40; 36B07-ZpGdbd in attP2)	Gerry Rubin and Aljoscha Nern, HHMI Janelia Research Campus	SS76489
w;Pdf-Red,Pdf-Gal4/cyo;+	Justin Blau, New York University	(85)
w;;UAS-NaChBac	Bloomington *Drosophila* Stock Center	RRID:BDSC_9468
yw;*UAS-hid/CyO*;+	Bloomington *Drosophila* Stock Center	RRID:BDSC_1557
w; UAS TeTxLC; +	Cahir O'Kane, University of Cambridge	RRID:BDSC_28838
w^{1118};+;+	Bloomington *Drosophila* Stock Center	RRID:BDSC_3605
w;;Pdf^{01}	Paul Taghert, Washington Univ. Med. School	(18)
LexAop2-Syb.GFPN146I.TEVT173V LexAop2QF2.V5.hSNAP25.HIVNES.Syx1A/CyO, 20XUAS-B3R.PEST UAS(B3RT.B2)BoNTA QUAS-mtdTomato-3xHA/TM6B, Tb1	Bloomington *Drosophila* Stock Center	RRID:BDSC 90825
Antibodies		
Mouse anti-PDF (1:3000 or 1:2000)	Developmental Studies Hybridoma Bank	
Rabbit anti-GFP (1:2000)	Thermo Fisher	A-11122
Rat anti-PER (1:500)	Orie Shafer, Indiana University Bloomington	
Rabbit anti-RFP (1:2000)	Rockland	#600-401-379-RTU
Chicken anti-GFP (1:2000)	Rockland	#600-901-215
Anti-mouse Alexa-488 (1:3000)	Thermo Fisher	A11029
Anti-rabbit Alexa-488 (1:3000)	Thermo Fisher	A48282
Anti-rat Alexa-568 (1:3000)	Thermo Fisher	A78946

Anti-rabbit Alexa-568 (1:3000)	Thermo Fisher	A11036
Anti-chicken Alexa-488 (1:3000)	Thermo Fisher	A11039
Software		
Fiji	http://fiji.sc	RRID: SCR_002285
PHASE	Open-source software: https://github.com/ajlopatkin/PHASE	(82)
MATLAB R2022b	MathWorks, Natick	RRID: SCR_001622
GraphPad Prism 9.0	GraphPad Software	RRID: SCR_002798
DAM FileScan	Trikinetics	
ClockLab	Actimetrics	RRID:SCR_014309
Chemicals		
Vectashield Mounting Medium	Vector Laboratories	#H-1000-10

Acknowledgments

We are grateful to Patrick Emery and members of the Fernández lab for helpful discussions and to Orie Shafer for comments on the manuscript, assistance on imaging, and providing access to the FV3000 microscope. We also thank the Janelia *FlyLight* Project Team for help with split-GAL4 screening and imaging, Justin Blau, Paul Taghert, and Cahir O'Kane for sharing fly lines, and Abhilash Lakshman for the code to obtain P(wake) and P(doze) values. Stocks obtained from the Bloomington *Drosophila* Stock Center (NIH P40OD018537) were used in this study. The mouse anti-PDF antibody was obtained from the Developmental Studies Hybridoma Bank, created by the NICHD of the NIH and maintained at The University of Iowa, Department of Biology, Iowa City, IA 52242, and the rat anti-PER antibody was donated by O. Shafer. This work was supported by a Beckman Foundation Scholarship to E.S-C, an NSF CAREER award (IOS-2239994) to M.P.F. and an NIH (R01NS118012) grant.

Conflict of interest statement

Authors declare that they have no competing interests.

459 **Figure legends**

460 **Fig. 1: SLP316 neurons are the main postsynaptic partner of the sLN$_v$s.**

461 (A-B) Connectomic mapping from the hemibrain dataset. (A) Map of top input/output neuronal groups
462 to/from the SLP316s and from the sLN$_v$s. The number of neurons in each group are indicated in
463 parenthesis if greater than one and reflected by circle size. Connection strength between cell types is
464 represented by arrow width and decreases in a clockwise direction for each connection type
465 (input/output). SLP232 likely corresponds to DN3s. (B) Strong shared inputs to, and (B') outputs of the
466 SLP316s (>10 synapses to/from at least two SLP316 neurons) with neuronal morphology shown above or
467 below. (C) Input synapses to, and output synapses of, the three SLP316 neurons (SLP316_R_1,
468 SLP316_R_2 and SLP316_R_3) shown in green, excluding synapses from neuron segments. Synapse
469 color corresponds to neuron color in (A) and (B) and all other synapses are shown in grey.

470

471 **Fig. 2: The SLP316 driver labels non-clock neurons that share functional synapses with the sLN$_v$s.**

472 (A-B) Representative confocal images of a brain from a 7-day old male fly (*SLP316>GFP)* stained with
473 antibodies against GFP (green) and PDF (magenta). (A) Whole brain, (B) Superior Lateral Protocerebrum
474 z-stack, and anterior (B') and posterior (B") single optical slices (step size 0.9 µm). (C) Quantification of
475 cell body count on the left hemisphere labelled by the *SLP316* driver in 7-day and 1-day old male and
476 female flies from three replicate experiments (n > 21 for each age/sex). (D) Representative confocal
477 images of a brain hemisphere of 6–7-day old male brains (*SLP316>GFP*) stained with antibodies against
478 GFP (green) and PER (magenta). (E-F) Representative confocal images of *SLP316-Gal4* and *Pdf-LexA*
479 driving expression of BAcTrace components. RFP signal can only be detected in the sLNvs. (E') sLN$_v$
480 dorsal termini show PDF and RFP expression. (E'') Cell bodies of sLN$_v$s and lLN$_v$s. (E''') sLN$_v$ cell
481 bodies plus dorsal projections show RFP signal, whereas the lLN$_v$s do not. (F) syb-GFP expression in the
482 small and large LN$_v$s in experimental brains. (G-H) Representative confocal images of *Pdf-LexA* driving
483 expression of BATrace components, without the SLP316-Gal4 driver. All scale bars are 50 µm.

484

485 **Fig. 3: Manipulation of the SLP316s modulates free-running period length**

486 (A) Representative double-plotted actograms, (B) free-running period calculated using the Chi-square
487 periodogram, and (C) percentage of rhythmic flies for control (*SLP316 split Gal4* and *UAS-NaChBac*)
488 and experimental (*SLP316>NaChBac*) flies. (D) Activity plot on the eighth day of free running, indicated
489 in (A) with yellow box. (E) Phase of activity from (D), calculated using a sine-fit of the waveform of
490 activity in CLOCKLAB. (F) Representative actograms, (G) free-running period and (H) percentage of
491 rhythmic flies for control (w*;UAS-hid;UAS-GFP* and w*;pUAS-tetx-LC-TNT;*) and experimental (*SLP316*
492 *>hid+GFP* or *SLP316>tetx-LC-TNT*) flies. (I) Free-running period, and (J) percentage of rhythmic flies

493 for control (*SLP316 split Gal4* and *;pUAS-tetx-LC-TNT;*) and experimental *(SLP316>tetx-LC-TNT*) flies.
494 (K) Activity plot and (L) phase of activity on the eighth day of free-running for control (*SLP316 split*
495 *Gal4* and *;pUAS-tetx-LC-TNT;*) and experimental *(SLP316 >tetx-LC-TNT*) flies. Actograms show 5 days
496 of LD followed by 9 days of DD. Flies were raised and activity-rest behavior recorded at 25°C. Rhythmic
497 power was calculated using the Chi-square periodogram in ClockLab using 30-minute activity bins, and
498 flies with a rhythmic power of 10 or greater were classified as rhythmic. Free-running period was
499 calculated for rhythmic flies using the Chi-square periodogram routine of ClockLab using 1-minute
500 activity bins. Statistical comparisons were conducted using the Kruskal-Wallis test followed by Dunn's
501 multiple comparisons test for free-running period and phase of activity, and using Fischer's exact test for
502 the number of rhythmic and arrhythmic flies. Data are plotted from three replicate experiments for each
503 genotype.
504
505 **Fig. 4: Silencing or eliminating SLP316 neurons does not affect the eclosion rhythm.** (A) Records
506 showing the time course of emergence of flies under DD conditions (left), their corresponding
507 autocorrelation analysis (middle), and periodicities (right). (B) Period of eclosion of populations of flies of
508 the indicated genotypes.
509
510 **Fig. 5: *Pdf* and SLP316 disruption have opposite effects on daytime activity and sleep quantities**
511 **under cold temperature**. (A-D) Activity and sleep phenotypes of *SLP316 >hid+GFP flies* during three
512 days of 12:12 LD at 18°C**.** Representative activity (A) and sleep (C) plots averaged for (*SLP316 split*
513 *Gal4* and *w;UAS-hid;UAS-GFP*) and experimental (*SLP316 >hid+GFP*) flies. Daytime (ZT0-12) (B)
514 activity counts and total sleep amount (D). (E-H) Activity and sleep phenotypes of *SLP316 >;tetx-LC-*
515 *TNT* flies and parental controls. Representative activity (E) and sleep (G) plots, and their respective
516 quantifications (F, H). (I-l) Activity and sleep phenotypes of for wild-type w^{1118} and pdf^{01} flies.
517 Representative activity (I) and sleep (K) plots, and total daytime activity counts (J) and sleep amount (L).
518 Flies were raised at 25°C and activity-rest behavior was recorded at 18°C. Statistical comparisons were
519 conducted using the Kruskal-Wallis test followed by Dunn's multiple comparisons test for comparisons
520 between three genotypes in (B), (D), (F) and (H), and using the Mann-Whitney test for comparisons
521 between two genotypes in (J) and (L). Data plotted are from two replicate experiments for (B), (D), (F)
522 and (H), and three replicate experiments for each genotype in (J) and (L).
523
524 **Fig. 6: Silencing or eliminating SLP316 neurons increases the amount of daytime sleep**
525 (A) Representative sleep plot averaged from three days of 12:12 LD at 25°C for control (*SLP316 split*
526 *Gal4* and *;UAS-hid;UAS-GFP*) and experimental (*SLP316 >;hid;GFP*) flies. (B) Total daytime sleep over

527 three days for each genotype. (C) Representative sleep plot and (D) total daytime sleep for control
528 (*SLP316-Gal4* and *;pUAS-tetx-LC-TNT;*) and experimental (*SLP316 >tetx-LC-TNT*) flies. (E) P(doze)
529 from the same three days of LD, plotted in three-hour for either control shown for controls, *SLP316 split*
530 *Gal4* and *;UAS-hid;UAS-GFP*), and experimental (*SLP316 >;hid;GFP*) flies. (F) Average P(doze)
531 throughout entire 3-day period. (G) P(doze) plot and (H) average P(doze) for control (*SLP316-Gal4* and
532 *;pUAS-tetx-LC-TNT;*) and experimental (*SLP316 >tetx-LC-TNT*) flies under same conditions. Sleep was
533 quantified in PHASE based on periods of inactivity of 5 minutes or more and plotted in (A) and (C) as
534 minutes of sleep per 30-minute bin. P(doze) was quantified in R using routines from the Griffith
535 Laboratory (66). Statistical comparisons were conducted using the Kruskal-Wallis test followed by
536 Dunn's multiple comparisons test. Data is plotted from four replicate experiments.
537
538 **Table 1. Summary of free running activity rhythms.** Activity analysis of the above genotypes at either
539 25˚C or 18˚C. Light conditions for each experiment were 12:12 LD-DD. For each genotype the number of
540 flies (n) is listed above. All flies were raised at 25˚C. ClockLab's χ-square periodogram analysis was used
541 to analyze rhythmicity, rhythmic power, and free-running period for each genotype. The percent
542 rhythmicity, along with the number of rhythmic flies (nR), the period in hours with the SEM, and the
543 rhythmic power with the SEM are indicated. Arrhythmic flies were not considered in the analysis.
544 Statistical analysis is included in Table S1.
545
546 **Supplementary Fig. 1:**
547 (A) Synapses from the four sLN_vs (red) onto the three SLP316 neurons above and below the main
548 branching point of the dorsal termini arborization in the hemibrain connectome. Synapses were counted
549 between each sLN_v and all their SLP316 targets. (B) Number of input synapses from, and output synapses
550 to, neurons classified by neuropil. (C) Connectomic mapping from FlyWire. Neuronal morphology of the
551 eight sLN_vs shown in red and their top post synaptic target cell type shown in green.
552
553 **Supplementary Fig. 2:**
554 (A) Overlay of the reconstructed SLP316 neuronal morphology from the hemibrain connectome
555 (magenta) and an LM image of SLP316 cells labeled using the SLP316 split-GAL4 line (SS76489). The
556 neuropil marker is anti-Brp (mAb NC82). (B) SLP316 cell body count in 7-day old vs 5-week-old male
557 flies. Statistical comparison was conducted using the Mann-Whitney test. (C) Representative confocal
558 image of an adult brain of *SLP316>mCD8GFP* flies stained with PDF (white), GFP (green), and RFP
559 (magenta) antibodies. Flies also carry a Hr38-Tomato transgene. Scale bar = 50 µm. (D) Quantification of
560 Hr38-Tomato reporter intensity in the sLN_vs (left) and SLP316 neurons (right). Scatterplots of RFP

561 staining intensities plotted at different time points over a 24-hr cycle on LD. Each dot represents the mean
562 RFP intensity value averaged over both hemispheres of one brain. The black lines are the best fit
563 cosine curves from the parameters that were extracted via COSINOR analysis.
564
565 **Supplementary Fig. 3:**
566 (A) Representative activity plot and (B) daytime activity counts from three days of 12:12 LD at 25°C for
567 male control (*SLP316-Gal4* and *w;;UAS-NaChBac*) and experimental (*SLP316>NaChBac*) flies. (C)
568 Morning and (D) evening phase and (E) evening peak area from the same days and genotypes, calculated
569 in PHASE using a 481-minute frame length and filter order of 2 to detect peaks. (F) Representative
570 activity plot, (G) daytime activity counts, (H) morning and (I) evening phase of activity, and (J) evening
571 peak area for male control (*SLP316-Gal4* and w*;UAS-hid;UAS-GFP*) and experimental
572 (*SLP316>hid+GFP*) flies. (K) Representative activity plot (L) daytime activity counts, (M) morning and
573 (N) evening phase of activity, and (O) evening peak area for male control (*SLP316-Gal4* and *w;pUAS-*
574 *tetx-LC-TNT;*) and experimental (*SLP316>tetx-LC-TNT*) flies. (P) Activity plot and (Q) phase of activity
575 from the eight day of free-running for control (*SLP316-Gal4* and *w;UAS-hid;UAS-GFP*) and
576 experimental (*SLP316>hid+GFP*) male flies. Statistical comparisons were conducted using the Kruskal-
577 Wallis test followed by Dunn's multiple comparisons test. Data from three replicate experiments for (B-E
578 and P-Q) and four replicate experiments for (G-J) and (L-O).
579
580 **Supplementary Fig. 4:**
581 (A) Free-running period for female control (*SLP316-Gal4* and *w;UAS-hid;UAS-GFP*) and experimental
582 (*SLP316 >hid+GFP*) flies. (B) Difference between male and female experimental (*SLP316 >hid+GFP*)
583 free-running periods, corrected by subtracting the average control free-running period from each
584 experimental value. (C) Free-running period for control (*SLP316 split Gal4* and *w;pUAS-tetx-LC-TNT;*)
585 and experimental (*SLP316 >tetx-LC-TNT*) female flies. (D) Difference between male and female
586 experimental (*SLP316>tetx-LC-TNT*) free-running periods, corrected as in (B). (E) Percent rhythmicity
587 for control (*SLP316-Gal4, w;UAS-hid;UAS-GFP,* and *w;pUAS-tetx-LC-TNT;*) and experimental
588 (*SLP316>hid+GFP* and *SLP316>tetx-LC-TNT*) female flies, with all relevant significance indicated. (F)
589 Representative sleep plot from three days of 12:12 LD at 25°C for control (*SLP316-Gal4* and *w;UAS-*
590 *hid;UAS-GFP*) and experimental (*SLP316 >hid+GFP*) female flies. (G) Total daytime sleep and (H)
591 nighttime sleep from plotted days for each genotype. (I) Representative sleep plot, (J) daytime sleep and
592 (K) nighttime sleep for control (*SLP316-Gal4* and *;pUAS-tetx-LC-TNT;*) and experimental (*SLP316*
593 *>tetx-LC-TNT*) flies under same conditions. Statistical comparisons were conducted using the Kruskal-

Wallis test followed by Dunn's multiple comparisons test. Data from one experiment for (A-E) and two replicate experiments for (G-H) and (J-K).

Supplementary Fig. 5:

(A) Records showing the time course of emergence of flies under DD conditions (left), their corresponding autocorrelation analysis (middle), and periodicities (right). (B) Period of eclosion of populations of flies of the indicated genotypes.

Supplementary Fig. 6:

(A) Nighttime activity and (B) nighttime sleep for control (*SLP316-Gal4* and *w;UAS-hid;UAS-GFP*) and experimental (*SLP316 >hid+GFP*) flies for three days of 12:12 LD at 18°C. (C) Nighttime activity and (D) nighttime sleep for control (*SLP316-Gal4* and *w;pUAS-tetx-LC-TNT;*) and experimental (*SLP316 >tetx-LC-TNT*) flies. (E) Nighttime activity and (F) nighttime sleep for wild-type w^{1118} and pdf^{01} flies.

Supplementary Fig. 7:

(A-B) P(wake) profiles (A) and values (B) plotted for three days of LD in three-hour bins shown for controls, *SLP316 split Gal4* and *w;UAS-hid;UAS-GFP*), and experimental (*SLP316 >hid + GFP*) flies. (C-D) P(wake) profiles (C) and values (D) plotted for three days of LD in three-hour bins shown for controls, *SLP316 split Gal4* and *w;pUAS-tetx-LC-TNT;*), and experimental (*SLP316 >TNT*) flies. P(wake) was quantified in R using routines from the Griffith Laboratory (66). Statistical comparisons were conducted using the Kruskal-Wallis test followed by Dunn's multiple comparisons test.

Table S1. Statistical analyses. Summary of statistical analyses used throughout the manuscript. All comparisons were conducted in GraphPad Prism, version 10.4.0

References

1. E. D. Herzog, Neurons and networks in daily rhythms. *Nat Rev Neurosci* **8**, 790-802 (2007).
2. D. K. Welsh, J. S. Takahashi, S. A. Kay, Suprachiasmatic nucleus: cell autonomy and network properties. *Annu Rev Physiol* **72**, 551-577 (2010).
3. M. H. Hastings, M. Brancaccio, E. S. Maywood, Circadian pacemaking in cells and circuits of the suprachiasmatic nucleus. *J Neuroendocrinol* **26**, 2-10 (2014).
4. E. S. Maywood, J. E. Chesham, J. A. O'Brien, M. H. Hastings, A diversity of paracrine signals sustains molecular circadian cycling in suprachiasmatic nucleus circuits. *Proceedings of the National Academy of Sciences* **108**, 14306-14311 (2011).
5. B. Ananthasubramaniam, E. D. Herzog, H. Herzel, Timing of neuropeptide coupling determines synchrony and entrainment in the mammalian circadian clock. *PLoS Comput Biol* **10**, e1003565 (2014).
6. P. H. Taghert, M. N. Nitabach, Peptide neuromodulation in invertebrate model systems. *Neuron* **76**, 82-97 (2012).
7. D. R. Nässel, M. Zandawala, Recent advances in neuropeptide signaling in Drosophila, from genes to physiology and behavior. *Prog Neurobiol* **179**, 101607 (2019).
8. N. Reinhard *et al.*, Synaptic connectome of the Drosophila circadian clock. *Nature Communications* **15**, 10392 (2024).
9. C. Helfrich-Förster, N. Reinhard, Mutual coupling of neurons in the circadian master clock: what we can learn from fruit flies. *Neurobiology of Sleep and Circadian Rhythms* https://doi.org/10.1016/j.nbscr.2025.100112, 100112 (2025).
10. C. Helfrich-Forster, The neuroarchitecture of the circadian clock in the brain of Drosophila melanogaster. *Microsc Res Tech* **62**, 94-102 (2003).
11. F. K. Schubert, N. Hagedorn, T. Yoshii, C. Helfrich-Forster, D. Rieger, Neuroanatomical details of the lateral neurons of Drosophila melanogaster support their functional role in the circadian system. *J Comp Neurol* **526**, 1209-1231 (2018).
12. C. Dubowy, A. Sehgal, Circadian Rhythms and Sleep in Drosophila melanogaster. *Genetics* **205**, 1373-1397 (2017).
13. C. Helfrich-Forster, Organization of endogenous clocks in insects. *Biochem Soc Trans* **33**, 957-961 (2005).
14. D. Ma *et al.*, A transcriptomic taxonomy of Drosophila circadian neurons around the clock. *eLife* **10**, e63056 (2021).
15. O. T. Shafer, C. Helfrich-Forster, S. C. Renn, P. H. Taghert, Reevaluation of Drosophila melanogaster's neuronal circadian pacemakers reveals new neuronal classes. *J Comp Neurol* **498**, 180-193 (2006).
16. O. T. Shafer *et al.*, Connectomic analysis of the Drosophila lateral neuron clock cells reveals the synaptic basis of functional pacemaker classes. *Elife* **11** (2022).
17. X. Liang, T. E. Holy, P. H. Taghert, Synchronous Drosophila circadian pacemakers display nonsynchronous Ca(2)(+) rhythms in vivo. *Science* **351**, 976-981 (2016).
18. S. C. Renn, J. H. Park, M. Rosbash, J. C. Hall, P. H. Taghert, A pdf neuropeptide gene mutation and ablation of PDF neurons each cause severe abnormalities of behavioral circadian rhythms in Drosophila. *Cell* **99**, 791-802 (1999).
19. J. H. Park *et al.*, Differential regulation of circadian pacemaker output by separate clock genes in Drosophila. *Proc Natl Acad Sci U S A* **97**, 3608-3613 (2000).
20. B. Grima, E. Chelot, R. Xia, F. Rouyer, Morning and evening peaks of activity rely on different clock neurons of the Drosophila brain. *Nature* **431**, 869-873 (2004).
21. D. Stoleru, Y. Peng, J. Agosto, M. Rosbash, Coupled oscillators control morning and evening locomotor behaviour of Drosophila. *Nature* **431**, 862-868 (2004).
22. T. Yoshii *et al.*, The neuropeptide pigment-dispersing factor adjusts period and phase of Drosophila's clock. *J Neurosci* **29**, 2597-2610 (2009).

23. Y. Peng, D. Stoleru, J. D. Levine, J. C. Hall, M. Rosbash, Drosophila free-running rhythms require intercellular communication. *PLoS Biol* **1**, E13 (2003).
24. X. Liang, T. E. Holy, P. H. Taghert, A Series of Suppressive Signals within the Drosophila Circadian Neural Circuit Generates Sequential Daily Outputs. *Neuron* **94**, 1173-1189 e1174 (2017).
25. I. Mertens *et al.*, PDF receptor signaling in Drosophila contributes to both circadian and geotactic behaviors. *Neuron* **48**, 213-219 (2005).
26. S. Hyun *et al.*, Drosophila GPCR Han is a receptor for the circadian clock neuropeptide PDF. *Neuron* **48**, 267-278 (2005).
27. B. C. Lear *et al.*, A G protein-coupled receptor, groom-of-PDF, is required for PDF neuron action in circadian behavior. *Neuron* **48**, 221-227 (2005).
28. H. A. D. Johard *et al.*, Peptidergic clock neurons in Drosophila: Ion transport peptide and short neuropeptide F in subsets of dorsal and ventral lateral neurons. *Journal of Comparative Neurology* **516**, 59-73 (2009).
29. C. G. Vecsey, N. Pirez, L. C. Griffith, The Drosophila neuropeptides PDF and sNPF have opposing electrophysiological and molecular effects on central neurons. *J Neurophysiol* **111**, 1033-1045 (2014).
30. Y. Shang *et al.*, Short neuropeptide F is a sleep-promoting inhibitory modulator. *Neuron* **80**, 171-183 (2013).
31. L. Frenkel *et al.*, Organization of Circadian Behavior Relies on Glycinergic Transmission. *Cell Rep* **19**, 72-85 (2017).
32. B. Hofbauer *et al.*, The neuropeptide pigment-dispersing factor signals independently of Bruchpilot-labelled active zones in daily remodelled terminals of Drosophila clock neurons. *Eur J Neurosci* **59**, 2665-2685 (2024).
33. M. K. Klose, M. P. Bruchez, D. L. Deitcher, E. S. Levitan, Temporally and spatially partitioned neuropeptide release from individual clock neurons. *Proc Natl Acad Sci U S A* **118** (2021).
34. S. T. Sweeney, K. Broadie, J. Keane, H. Niemann, C. J. O'Kane, Targeted expression of tetanus toxin light chain in Drosophila specifically eliminates synaptic transmission and causes behavioral defects. *Neuron* **14**, 341-351 (1995).
35. A. R. Iyer *et al.*, The Circadian Neuropeptide PDF has Sexually Dimorphic Effects on Activity Rhythms. *bioRxiv* 10.1101/2024.01.31.578273 (2024).
36. M. Kaneko, J. H. Park, Y. Cheng, P. E. Hardin, J. C. Hall, Disruption of synaptic transmission or clock-gene-product oscillations in circadian pacemaker cells of Drosophila cause abnormal behavioral rhythms. *J Neurobiol* **43**, 207-233 (2000).
37. M. P. Brown *et al.*, A subclass of evening cells promotes the switch from arousal to sleep at dusk. *bioRxiv* 10.1101/2023.08.28.555147 (2023).
38. M. P. Fernandez *et al.*, Sites of Circadian Clock Neuron Plasticity Mediate Sensory Integration and Entrainment. *Curr Biol* **30**, 2225-2237 e2225 (2020).
39. F. Guo, X. Chen, M. Rosbash, Temporal calcium profiling of specific circadian neurons in freely moving flies. *Proc Natl Acad Sci U S A* **114**, E8780-E8787 (2017).
40. A. Lamaze, R. Stanewsky, DN1p or the "Fluffy" Cerberus of Clock Outputs. *Front Physiol* **10**, 1540 (2019).
41. B. Collins, Elizabeth A. Kane, David C. Reeves, Myles H. Akabas, J. Blau, Balance of Activity between LNvs and Glutamatergic Dorsal Clock Neurons Promotes Robust Circadian Rhythms in Drosophila. *Neuron* **74**, 706-718 (2012).
42. J. Majercak, D. Sidote, P. E. Hardin, I. Edery, How a circadian clock adapts to seasonal decreases in temperature and day length. *Neuron* **24**, 219-230 (1999).
43. P. Lamba, L. E. Foley, P. Emery, Neural network interactions modulate CRY-dependent photoresponses in Drosophila. *The Journal of Neuroscience* 10.1523/jneurosci.2259-17.2018, 2259-2217 (2018).

44. A. Chatterjee *et al.*, Reconfiguration of a Multi-oscillator Network by Light in the Drosophila Circadian Clock. *Curr Biol* **28**, 2007-2017 e2004 (2018).
45. Y. Zhang, Y. Liu, D. Bilodeau-Wentworth, P. E. Hardin, P. Emery, Light and temperature control the contribution of specific DN1 neurons to Drosophila circadian behavior. *Curr Biol* **20**, 600-605 (2010).
46. K. M. Parisky, J. L. Agosto Rivera, N. C. Donelson, S. Kotecha, L. C. Griffith, Reorganization of Sleep by Temperature in Drosophila Requires Light, the Homeostat, and the Circadian Clock. *Curr Biol* **26**, 882-892 (2016).
47. C. Kistenpfennig *et al.*, A New Rhodopsin Influences Light-dependent Daily Activity Patterns of Fruit Flies. *J Biol Rhythms* **32**, 406-422 (2017).
48. L. K. Scheffer *et al.*, A connectome and analysis of the adult Drosophila central brain. *Elife* **9** (2020).
49. S. Dorkenwald *et al.*, Neuronal wiring diagram of an adult brain. *Nature* **634**, 124-138 (2024).
50. N. Eckstein *et al.*, Neurotransmitter classification from electron microscopy images at synaptic sites in Drosophila melanogaster. *Cell* **187**, 2574-2594.e2523 (2024).
51. O. T. Shafer, M. Rosbash, J. W. Truman, Sequential nuclear accumulation of the clock proteins period and timeless in the pacemaker neurons of Drosophila melanogaster. *J Neurosci* **22**, 5946-5954 (2002).
52. Z. Zhu *et al.*, A gene expression program activated by neuronal inactivity. *bioRxiv* 10.1101/636878, 636878 (2024).
53. D. G. Gundermann, S. Lymer, J. Blau, A rapid and dynamic role for FMRP in the plasticity of adult neurons. *bioRxiv* 10.1101/2023.09.01.555985 (2023).
54. S. Cachero *et al.*, BAcTrace, a tool for retrograde tracing of neuronal circuits in Drosophila. *Nature Methods* **17**, 1254-1261 (2020).
55. F. Lehmann-Horn, K. Jurkat-Rott, Voltage-gated ion channels and hereditary disease. *Physiol Rev* **79**, 1317-1372 (1999).
56. M. N. Nitabach *et al.*, Electrical hyperexcitation of lateral ventral pacemaker neurons desynchronizes downstream circadian oscillators in the fly circadian circuit and induces multiple behavioral periods. *J Neurosci* **26**, 479-489 (2006).
57. D. Stoleru, Y. Peng, P. Nawathean, M. Rosbash, A resetting signal between Drosophila pacemakers synchronizes morning and evening activity. *Nature* **438**, 238-242 (2005).
58. Z. Yao, A. J. Bennett, J. L. Clem, O. T. Shafer, The Drosophila Clock Neuron Network Features Diverse Coupling Modes and Requires Network-wide Coherence for Robust Circadian Rhythms. *Cell Rep* **17**, 2873-2881 (2016).
59. M. Selcho *et al.*, Central and peripheral clocks are coupled by a neuropeptide pathway in Drosophila. *Nature Communications* **8**, 15563 (2017).
60. C. Wegener, E. Amini, J. Cavieres-Lepe, J. Ewer, Neuronal and endocrine mechanisms underlying the circadian gating of eclosion: insights from Drosophila. *Curr Opin Insect Sci* **66**, 101286 (2024).
61. C. Helfrich-Forster, Development of pigment-dispersing hormone-immunoreactive neurons in the nervous system of Drosophila melanogaster. *J Comp Neurol* **380**, 335-354 (1997).
62. S. Hidalgo, M. Anguiano, C. A. Tabuloc, J. C. Chiu, Seasonal cues act through the circadian clock and pigment-dispersing factor to control EYES ABSENT and downstream physiological changes. *Curr Biol* **33**, 675-687 e675 (2023).
63. K. M. Parisky *et al.*, PDF cells are a GABA-responsive wake-promoting component of the Drosophila sleep circuit. *Neuron* **60**, 672-682 (2008).
64. P. J. Shaw, C. Cirelli, R. J. Greenspan, G. Tononi, Correlates of sleep and waking in Drosophila melanogaster. *Science* **287**, 1834-1837 (2000).
65. J. C. Hendricks *et al.*, Rest in Drosophila is a sleep-like state. *Neuron* **25**, 129-138 (2000).
66. T. D. Wiggin *et al.*, Covert sleep-related biological processes are revealed by probabilistic analysis in Drosophila. *Proc Natl Acad Sci U S A* **117**, 10024-10034 (2020).

67. P. H. Taghert, O. T. Shafer, Mechanisms of clock output in the Drosophila circadian pacemaker system. *J Biol Rhythms* **21**, 445-457 (2006).
68. O. T. Shafer *et al.*, Widespread receptivity to neuropeptide PDF throughout the neuronal circadian clock network of Drosophila revealed by real-time cyclic AMP imaging. *Neuron* **58**, 223-237 (2008).
69. N. Pirez, S. G. Bernabei-Cornejo, M. Fernandez-Acosta, J. M. Duhart, M. F. Ceriani, Contribution of non-circadian neurons to the temporal organization of locomotor activity. *Biol Open* **8** (2019).
70. A. Ehrlich *et al.*, Tango-seq: overlaying transcriptomics on connectomics to identify neurons downstream of Drosophila clock neurons. *bioRxiv* 10.1101/2024.05.22.595372 (2024).
71. M. P. Fernandez, J. Berni, M. F. Ceriani, Circadian remodeling of neuronal circuits involved in rhythmic behavior. *PLoS Biol* **6**, e69 (2008).
72. A. F. Neitz, B. M. Carter, M. F. Ceriani, M. H. Ellisman, H. O. de la Iglesia, Suprachiasmatic nucleus VIPergic fibers show a circadian rhythm of expansion and retraction. *Current Biology* **34**, 4056-4061.e4052 (2024).
73. A. Sivachenko, Y. Li, K. C. Abruzzi, M. Rosbash, The transcription factor Mef2 links the Drosophila core clock to Fas2, neuronal morphology, and circadian behavior. *Neuron* **79**, 281-292 (2013).
74. M. Sekiguchi *et al.*, A Detailed Re-Examination of the Period Gene Rescue Experiments Shows That Four to Six Cryptochrome-Positive Posterior Dorsal Clock Neurons (DN(1p)) of Drosophila melanogaster Can Control Morning and Evening Activity. *J Biol Rhythms* **39**, 463-483 (2024).
75. A. Chatterjee, J. De, B. Martin, E. Chélot, F. Rouyer, Neuropeptide Dynamics Coordinate Layered Plasticity Mechanisms Adapting Drosophila Circadian Behavior to Changing Environment. *bioRxiv* 10.1101/2024.10.15.618497, 2024.2010.2015.618497 (2024).
76. Y. Fujiwara *et al.*, The CCHamide1 Neuropeptide Expressed in the Anterior Dorsal Neuron 1 Conveys a Circadian Signal to the Ventral Lateral Neurons in Drosophila melanogaster. *Front Physiol* **9**, 1276 (2018).
77. M. H. Alpert *et al.*, A Circuit Encoding Absolute Cold Temperature in Drosophila. *Curr Biol* **30**, 2275-2288 e2275 (2020).
78. F. Guo *et al.*, Circadian neuron feedback controls the Drosophila sleep--activity profile. *Nature* **536**, 292-297 (2016).
79. G. W. Meissner *et al.* (2025) A split-GAL4 driver line resource for Drosophila neuron types. (eLife Sciences Publications, Ltd).
80. P. Schlegel *et al.*, Whole-brain annotation and multi-connectome cell typing of Drosophila. *Nature* **634**, 139-152 (2024).
81. C. Pfeiffenberger, B. C. Lear, K. P. Keegan, R. Allada, Processing circadian data collected from the Drosophila Activity Monitoring (DAM) System. *Cold Spring Harb Protoc* **2010**, pdb prot5519 (2010).
82. J. L. Persons *et al.*, PHASE: An Open-Source Program for the Analysis of DrosophilaPhase, Activity, and Sleep Under Entrainment. *J Biol Rhythms* **37**, 455-467 (2022).
83. J. Cavieres-Lepe *et al.*, Timed receptor tyrosine kinase signaling couples the central and a peripheral circadian clock in Drosophila. *Proc Natl Acad Sci U S A* **121**, e2308067121 (2024).
84. J. D. Levine, P. Funes, H. B. Dowse, J. C. Hall, Signal analysis of behavioral and molecular cycles. *BMC Neuroscience* **3**, 1 (2002).
85. M. Ruben, M. D. Drapeau, D. Mizrak, J. Blau, A mechanism for circadian control of pacemaker neuron excitability. *J Biol Rhythms* **27**, 353-364 (2012).

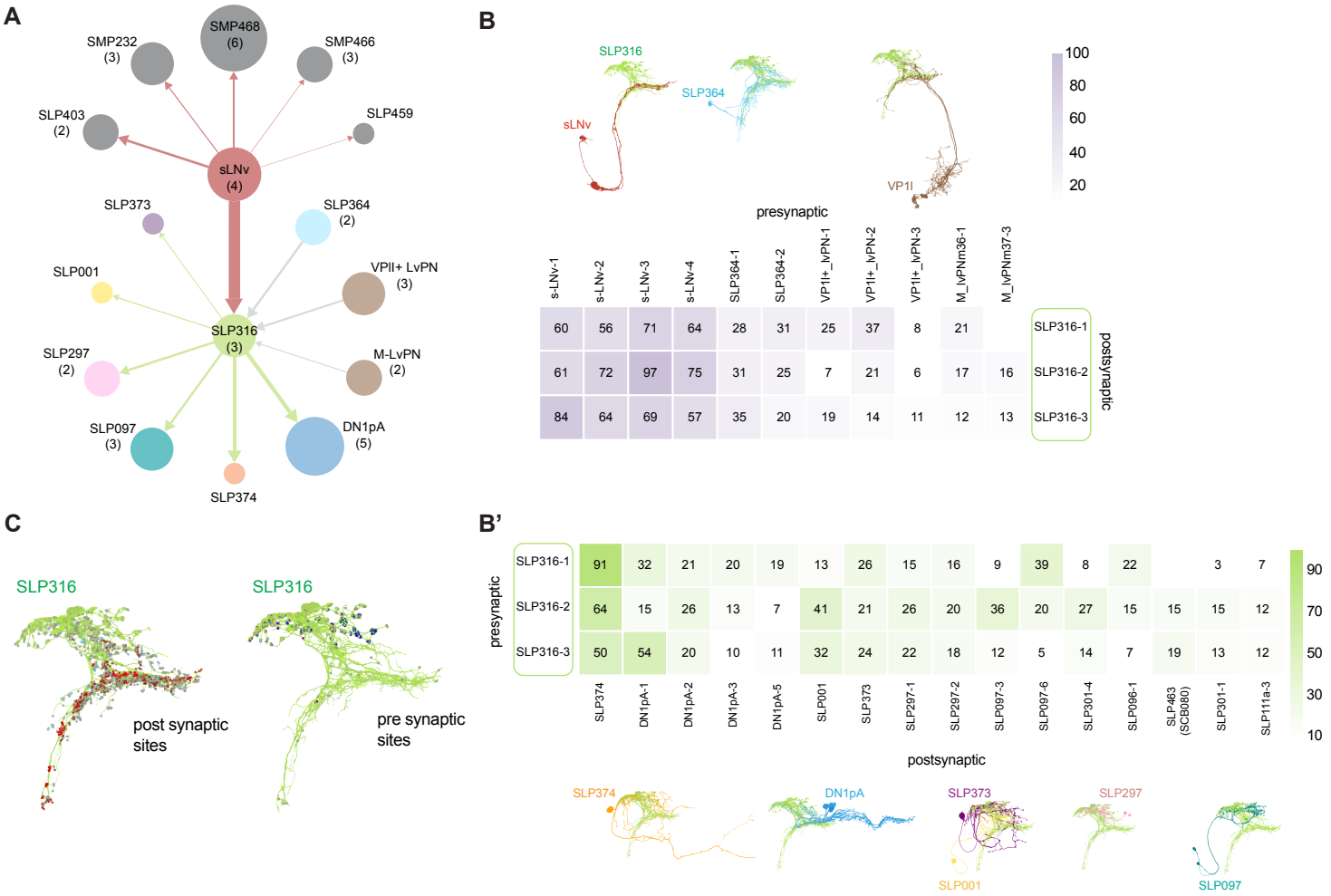
A
SMP468 (6)
SMP232 (3)
SMP466 (3)
SLP403 (2)
SLP459
sLNv (4)
SLP373
SLP364 (2)
SLP001
VPII+ LvPN (3)
SLP316 (3)
SLP297 (2)
M-LvPN (2)
SLP097 (3)
DN1pA (5)
SLP374
B
SLP316
SLP364
sLNv
VP1l
100
80
60
40
20
presynaptic
s-LNv-1 s-LNv-2 s-LNv-3 s-LNv-4 SLP364-1 SLP364-2 VP1l+_lvPN-1 VP1l+_lvPN-2 VP1l+_lvPN-3 M_lvPNm36-1 M_lvPNm37-3
SLP316-1 60 56 71 64 28 31 25 37 8 21
SLP316-2 61 72 97 75 31 25 7 21 6 17 16
SLP316-3 84 64 69 57 35 20 19 14 11 12 13
postsynaptic
C
SLP316
post synaptic sites
SLP316
pre synaptic sites
B'
presynaptic
SLP316-1 91 32 21 20 19 13 26 15 16 9 39 8 22 3 7
SLP316-2 64 15 26 13 7 41 21 26 20 36 20 27 15 15 15 12
SLP316-3 50 54 20 10 11 32 24 22 18 12 5 14 7 19 13 12
SLP374 DN1pA-1 DN1pA-2 DN1pA-3 DN1pA-5 SLP001 SLP373 SLP297-1 SLP297-2 SLP097-3 SLP097-6 SLP301-4 SLP096-1 SLP463 (SCB080) SLP301-1 SLP111a-3
postsynaptic
90
70
50
30
10
SLP374
DN1pA
SLP373
SLP297
SLP001
SLP097

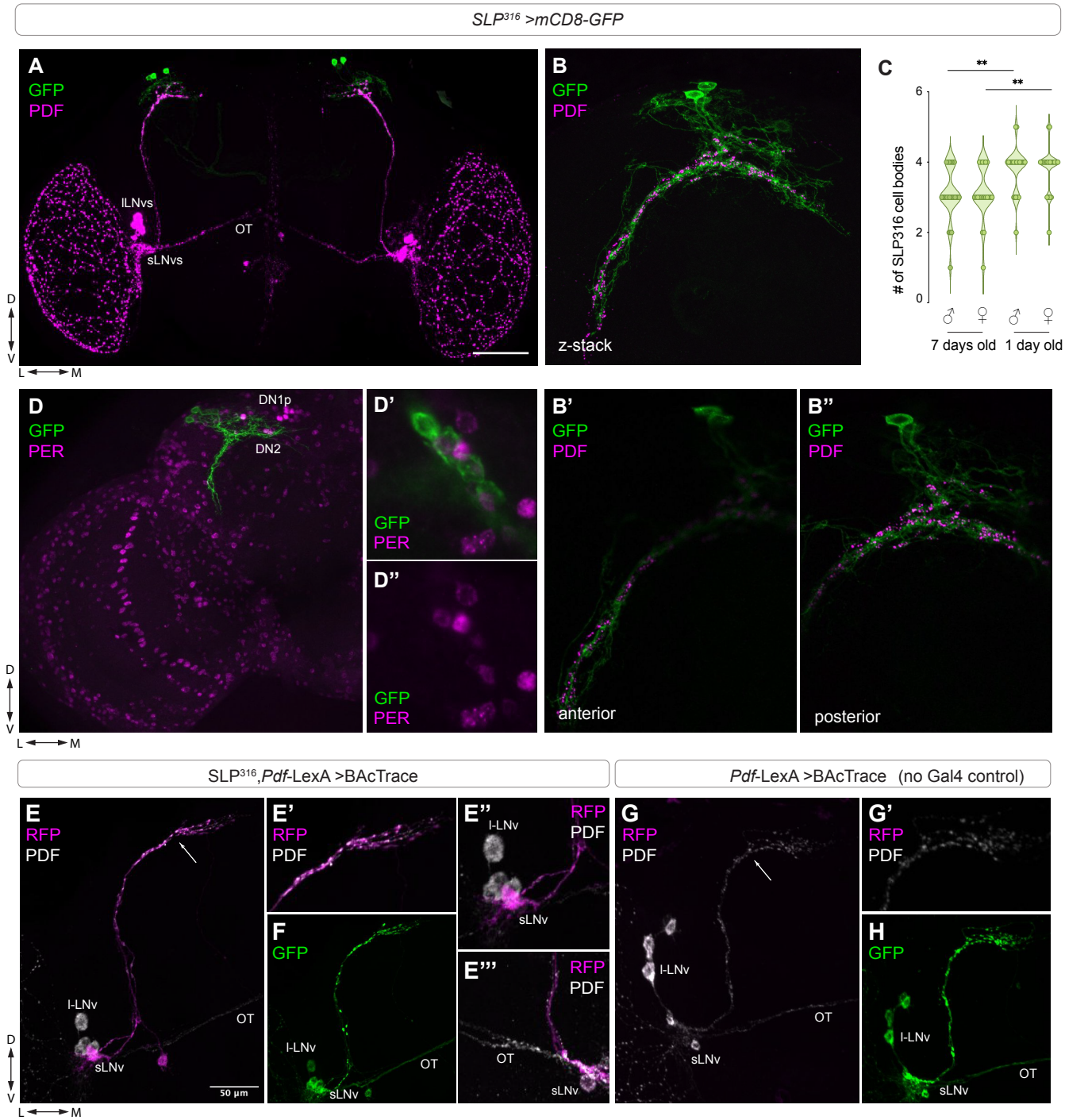
SLP316 >mCD8-GFP
A
GFP
PDF
lLNvs
OT
sLNvs
D
V
L
M
B
GFP
PDF
z-stack
C
**
**
6
4
2
0
# of SLP316 cell bodies
♂
♀
♂
♀
7 days old
1 day old
D
GFP
PER
DN1p
DN2
D'
GFP
PER
D''
GFP
PER
B'
GFP
PDF
anterior
B''
GFP
PDF
posterior
SLP316,Pdf-LexA >BAcTrace
Pdf-LexA >BAcTrace (no Gal4 control)
E
RFP
PDF
l-LNv
OT
sLNv
50 µm
E'
RFP
PDF
F
GFP
l-LNv
OT
sLNv
E''
l-LNv
RFP
PDF
sLNv
E'''
RFP
PDF
OT
sLNv
G
RFP
PDF
l-LNv
OT
sLNv
G'
RFP
PDF
H
GFP
l-LNv
OT
sLNv

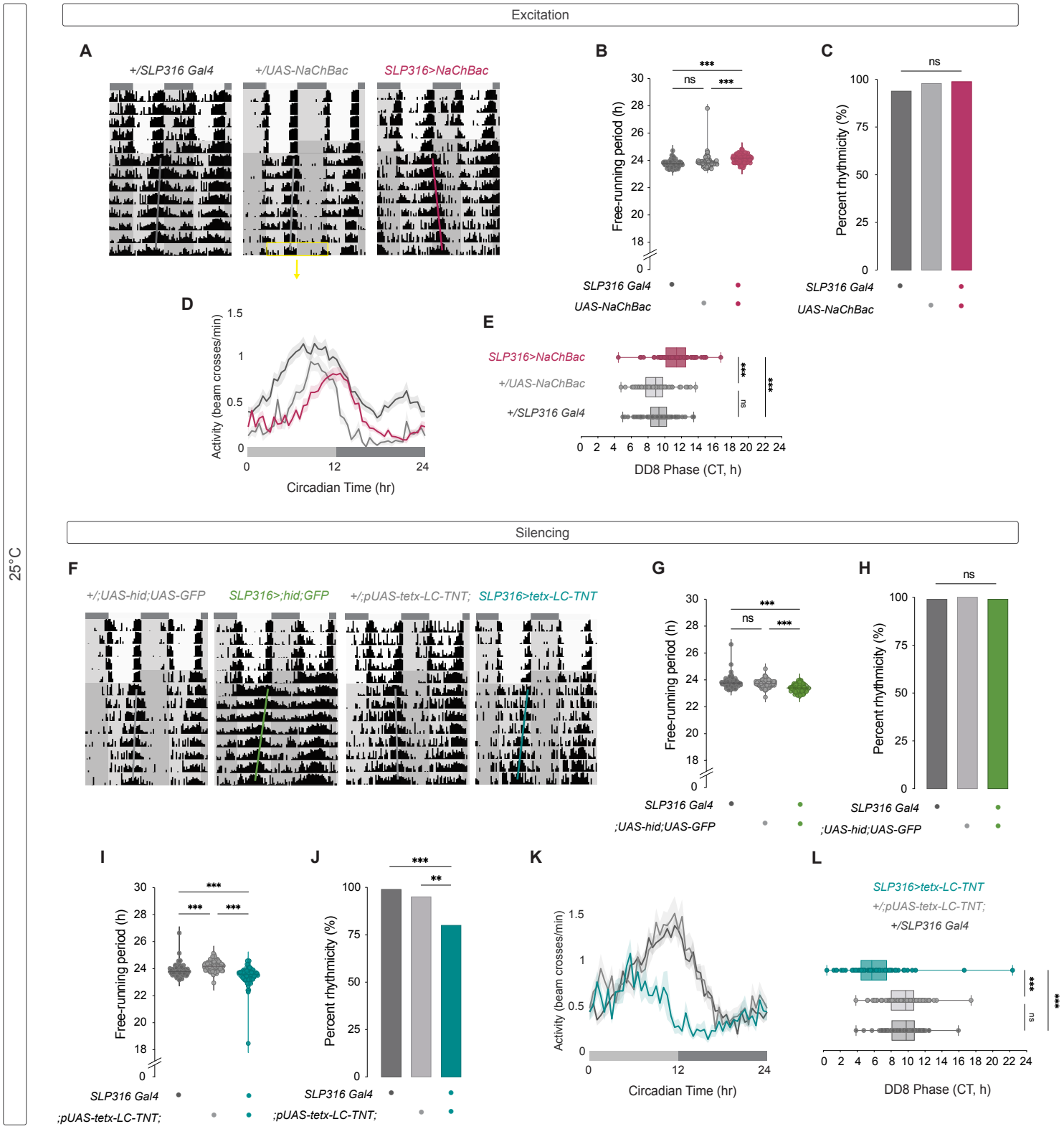
25°C
Excitation
A
+/SLP316 Gal4
+/UAS-NaChBac
SLP316>NaChBac
B
Free-running period (h)
***
ns
***
SLP316 Gal4
UAS-NaChBac
C
Percent rhythmicity (%)
ns
SLP316 Gal4
UAS-NaChBac
D
Activity (beam crosses/min)
Circadian Time (hr)
E
SLP316>NaChBac
+/UAS-NaChBac
+/SLP316 Gal4
***
ns
***
DD8 Phase (CT, h)
Silencing
F
+/;UAS-hid;UAS-GFP
SLP316>;hid;GFP
+/;pUAS-tetx-LC-TNT;
SLP316>tetx-LC-TNT
G
Free-running period (h)
***
ns
***
SLP316 Gal4
;UAS-hid;UAS-GFP
H
Percent rhythmicity (%)
ns
SLP316 Gal4
;UAS-hid;UAS-GFP
I
Free-running period (h)
***
***
***
SLP316 Gal4
;pUAS-tetx-LC-TNT;
J
Percent rhythmicity (%)
***
**
SLP316 Gal4
;pUAS-tetx-LC-TNT;
K
Activity (beam crosses/min)
Circadian Time (hr)
L
SLP316>tetx-LC-TNT
+/;pUAS-tetx-LC-TNT;
+/SLP316 Gal4
***
ns
***
DD8 Phase (CT, h)

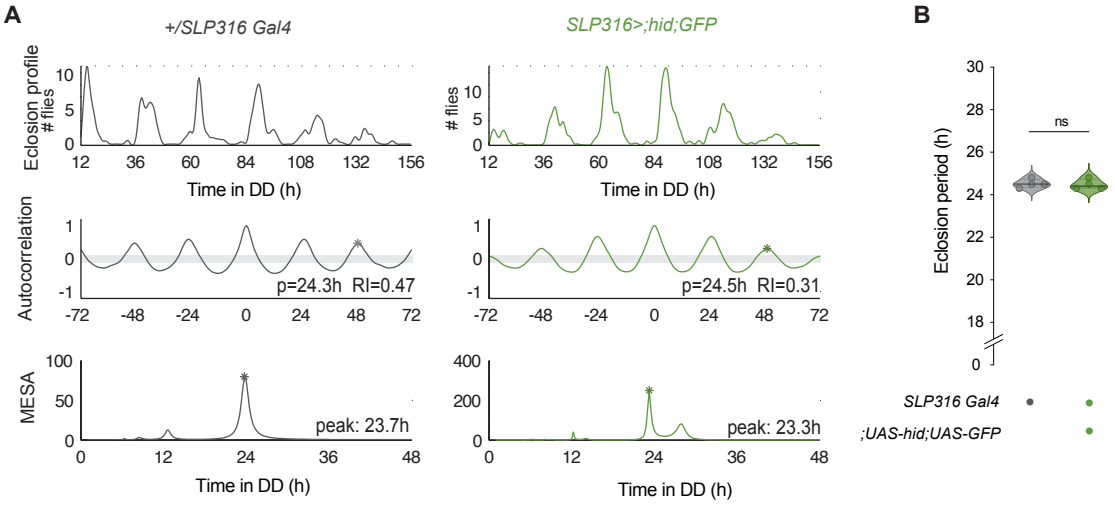
A
+/SLP316 Gal4
SLP316>;hid;GFP
Eclosion profile
flies
Time in DD (h)
Autocorrelation
p=24.3h RI=0.47
p=24.5h RI=0.31
MESA
peak: 23.7h
peak: 23.3h
B
Eclosion period (h)
ns
SLP316 Gal4
;UAS-hid;UAS-GFP

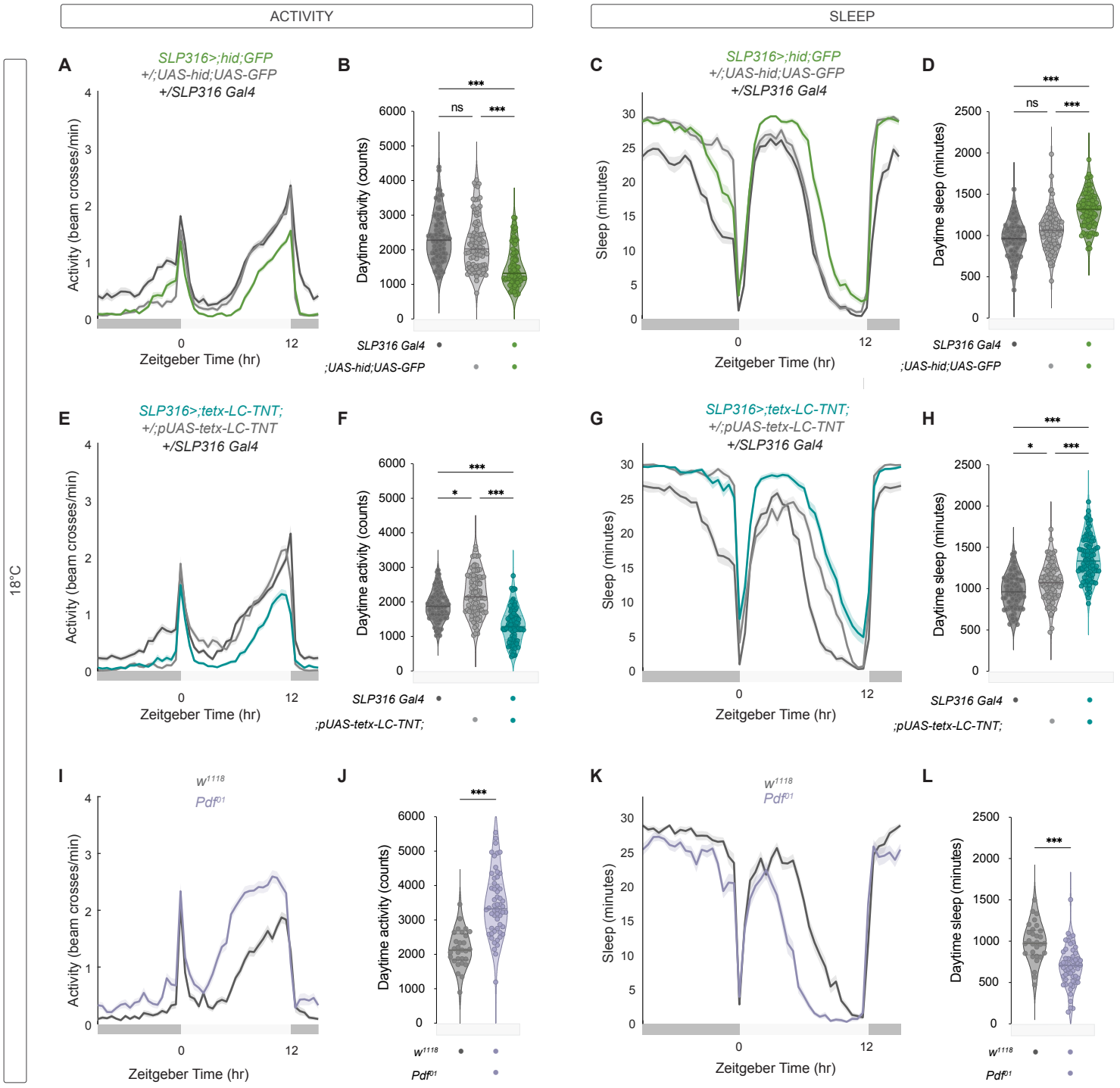
ACTIVITY
SLEEP
18°C
A
SLP316>;hid;GFP
+/;UAS-hid;UAS-GFP
+/SLP316 Gal4
Activity (beam crosses/min)
Zeitgeber Time (hr)
B
Daytime activity (counts)
ns
***
SLP316 Gal4
;UAS-hid;UAS-GFP
C
Sleep (minutes)
D
Daytime sleep (minutes)
E
SLP316>;tetx-LC-TNT;
+/;pUAS-tetx-LC-TNT
+/SLP316 Gal4
*
;pUAS-tetx-LC-TNT;
F
G
H
I
w1118
Pdf01
J
K
L

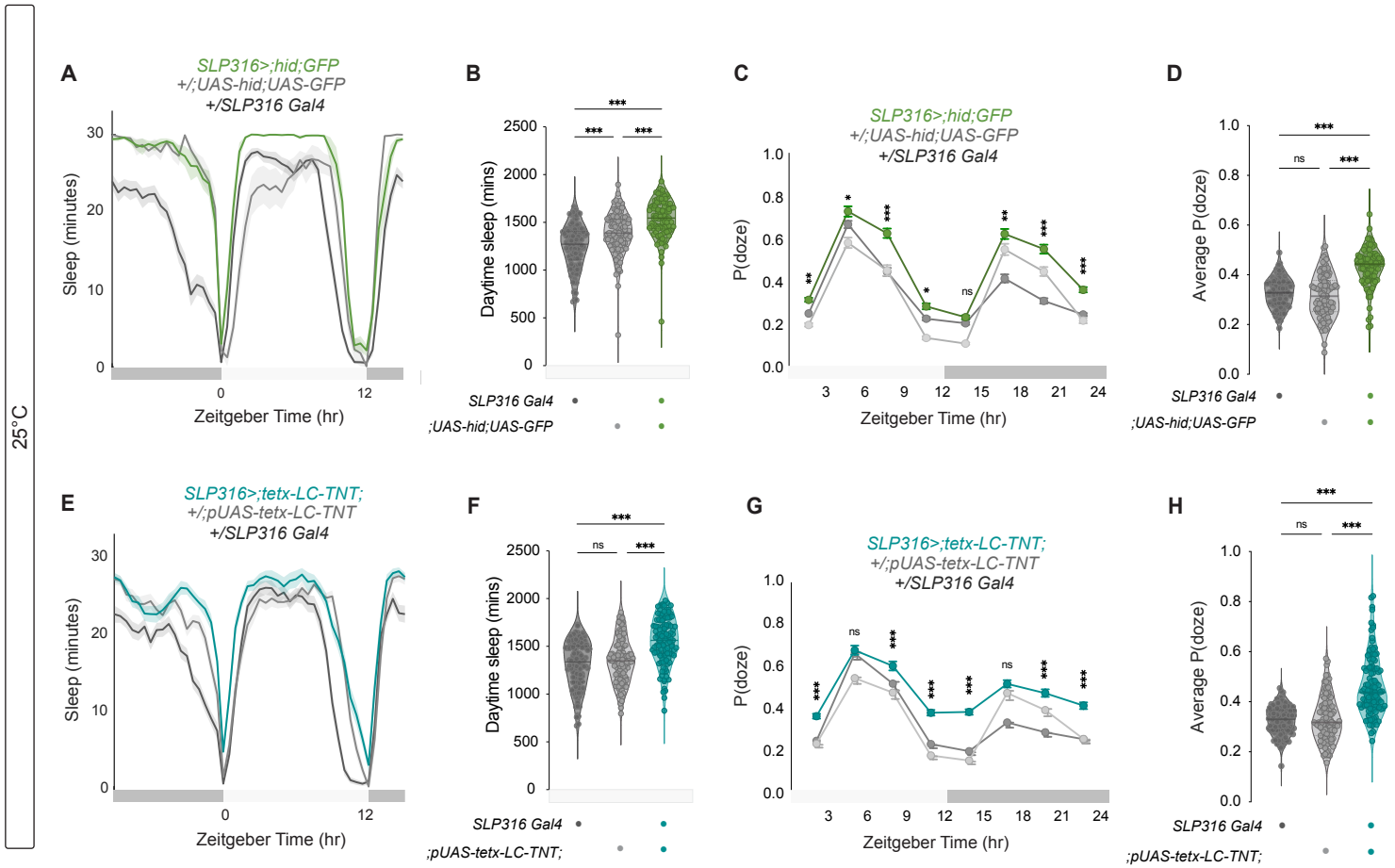
25°C
A
SLP316>;hid;GFP
+/;UAS-hid;UAS-GFP
+/SLP316 Gal4
Sleep (minutes)
Zeitgeber Time (hr)
B
Daytime sleep (mins)
SLP316 Gal4
;UAS-hid;UAS-GFP
C
SLP316>;hid;GFP
+/;UAS-hid;UAS-GFP
+/SLP316 Gal4
P(doze)
Zeitgeber Time (hr)
D
Average P(doze)
SLP316 Gal4
;UAS-hid;UAS-GFP
E
SLP316>;tetx-LC-TNT;
+/;pUAS-tetx-LC-TNT
+/SLP316 Gal4
Sleep (minutes)
Zeitgeber Time (hr)
F
Daytime sleep (mins)
SLP316 Gal4
;pUAS-tetx-LC-TNT;
G
SLP316>;tetx-LC-TNT;
+/;pUAS-tetx-LC-TNT
+/SLP316 Gal4
P(doze)
Zeitgeber Time (hr)
H
Average P(doze)
SLP316 Gal4
;pUAS-tetx-LC-TNT;

Table 1. Summary of free running activity rhythms at 25˚C and 18˚C.

Temperature: 25˚C					
Genotype	Sex	Number of Flies (n)	% Rhythmicity (nR)	Period (h) ± SEM	Rhythmic Power ± SEM
;Pdf-Red,Pdf-Gal4;	M	90	100 (90)	24.57 ± 0.04	148.3 ± 6.06
;pUAS-tetx-LC-TNT;	M	113	96.46 (109)	24.11 ± 0.04	91.38 ± 4.75
;Pdf-Red,Pdf-Gal4; > ;tetx-LC-TNT;	M	76	78.95 (60)	24.99 ± 0.11	64.58 ± 5.45
SLP316 split Gal4	M	170	95.88 (163)	23.82 ± 0.03	117.4 ± 4.14
NaChBac	M	73	98.63 (72)	23.91 ± 0.06	172.0 ± 5.82
SLP316 > NaChBac	M	69	98.55 (68)	24.13 ± 0.04	171.0 ± 5.30
;UAS-hid;UAS-GFP	M	76	100 (76)	23.73 ± 0.03	167.9 ± 5.39
SLP316 > ;hid;GFP	M	68	98.80 (82)	23.38 ± 0.04	144.5 ± 6.98
SLP316 > ;tetx-LC-TNT;	M	85	80.0 (68)	23.47 ± 0.09	41.02 ± 3.46
SLP316 split Gal4	F	31	80.65 (25)	24.41 ± 0.12	89.78 ± 11.06
;UAS-hid;UAS-GFP	F	32	100 (32)	24.39 ± 0.06	174.5 ± 8.34
SLP316 > ;hid;GFP	F	32	100 (32)	24.26 ± 0.26	169.1 ± 11.20
;pUAS-tetx-LC-TNT;	F	29	93.10 (27)	25.14 ± 0.34	117.4 ± 10.96
SLP316 > ;tetx-LC-TNT;	F	31	96.77 (30)	24.25 ± 0.07	131.1 ± 7.69

Temperature: 18˚C					
Genotype	Sex	Number of Flies (n)	% Rhythmicity (nR)	Period (h) ± SEM	Rhythmic Power ± SEM
SLP316 split Gal4	M	160	97.50 (156)	23.86 ± 0.11	81.45 ± 2.87
NaChBac	M	32	100 (32)	23.72 ± 0.06	100.7 ± 5.74
SLP316 > NaChBac	M	32	100 (32)	23.70 ± 0.07	106.5 ± 6.93
;UAS-hid;UAS-GFP	M	94	100 (94)	23.78 ± 0.03	121.5 ± 4.91
SLP316 > ;hid;GFP	M	92	89.13 (82)	23.53 ± 0.18	67.05 ± 4.41
;pUAS-tetx-LC-TNT;	M	94	79.79 (75)	23.83 ± 0.18	49.49 ± 3.57
SLP316 > ;tetx-LC-TNT;	M	95	68.42 (65)	23.45 ± 0.17	36.00 ± 2.84
Pdf01	M	31	93.55 (29)	23.88 ± 0.04	63.02 ± 6.584
SLP316 split Gal4	F	63	84.13 (53)	24.12 ± 0.18	79.16 ± 6.03
;UAS-hid;UAS-GFP	F	25	84.00(21)	24.15 ± 0.13	66.93 ± 7.93
SLP316 > ;hid;GFP	F	26	92.31 (24)	23.54 ± 0.56	84.16 ± 9.95
;pUAS-tetx-LC-TNT;	F	64	93.75 (60)	24.29 ± 0.06	103.9 ± 6.31
SLP316 > ;tetx-LC-TNT;	F	58	91.38 (53)	23.75 ± 0.09	82.40 ± 5.64